

# **Friction measurements of InAs nanowires on SiO<sub>2</sub>, silanised SiO<sub>2</sub> and Si<sub>3</sub>N<sub>4</sub> by AFM manipulation**

**Gabriela Conache<sup>1,2</sup>, Struan Gray<sup>1</sup>, Aline Ribayrol<sup>1</sup>, Linus E Fröberg<sup>1</sup>, Lars Samuelson<sup>1</sup>, Håkan Pettersson<sup>2</sup>, and Lars Montelius<sup>1</sup>**

<sup>1</sup> Lund University, Solid State Physics/Nanometer Consortium, Lund, Sweden

<sup>2</sup> Halmstad University, Halmstad, Sweden

## **Abstract**

We have investigated friction between InAs nanowires and three different substrates: SiO<sub>2</sub>, silanised SiO<sub>2</sub> and Si<sub>3</sub>N<sub>4</sub>. The nanowires were pushed laterally with the tip of an AFM and the friction force per unit length for both static and sliding friction was deduced from their resulting curvature. On all three substrates thick wires showed a difference between sliding and static friction of up to three orders of magnitude. In addition, the three surfaces all showed a transition to stick-slip motion below a diameter of around 40 nm. That hydrophobic and hydrophilic substrates are so similar indicates that a condensed water layer does not strongly influence our results.

## Introduction

We recently reported a technique that allows measurements of the friction between extended contacts in the mesoscopic length scale, and which bridges the gap between point-contact studies of friction at the atomic scale and macroscopic phenomena [1,2]. The technique uses AFM manipulation of nanowires lying on a substrate surface to force them into an elastically strained shape. The curvature of the wire after manipulation is determined by an interplay between internal restoring forces and friction with the substrate, and after suitable manipulations it is possible to provide separate measures of both sliding and static friction.

The technique measures a distributed friction along an extended length of the nanowires. The contact geometry is well characterised for single-crystal nanowires, and their intrinsic attraction to the surface is perturbed only in a very localised region by the presence of the AFM tip. We can therefore study a well-characterised contact which is point contact-like across the wire but which is up to several microns in length along the wire axis. The intrinsic attraction of the wires to the surface determines the normal force across the contact and extensive characterisation of the AFM tip and cantilever is not therefore necessary.

In Ref. 2 we showed how InAs nanowires on  $\text{Si}_3\text{N}_4$  substrates displayed a variety of behaviours, some of which seemed characteristic of atomic-scale friction and some of which were more macroscopic in character. Large wires showed a considerable difference in the coefficients for sliding and static friction, a feature which is usually associated with the atomic scale. Contrarily, the static friction varied with the nanowire diameter in a way that suggested a macroscopic model in terms of an ensemble of micro-asperities becoming active at different contact pressures, which might be more appropriate. Finally, there was a transition to stick-slip motion at a nanowire diameter of around 40 nm.

In the present paper we have investigated InAs nanowires on a variety of substrates in order to assess the general applicability of our experimental technique, and to try and shed light on the important parameters governing the observed friction behaviour. The friction force per unit length was measured for both static and sliding friction for InAs wires on  $\text{SiO}_2$ , silanised  $\text{SiO}_2$  and  $\text{Si}_3\text{N}_4$ . The three substrates do show different levels of friction, although the differences were not as dramatic as might be expected from their macroscopic reputations. By comparing results from the strongly hydrophobic silanised surface with those obtained on the hydrophilic oxide and nitride surfaces we show that the absorbed water layer on the hydrophobic surfaces does not greatly influence our results. Most importantly, the patterns and trends in the friction values as a function of nanowire diameter seen in Ref. 2 were reproduced on all three substrates, indicating that they are of fundamental character and not just particular to a single substrate.

## Experimental Details

The InAs nanowires were fabricated by Chemical Beam Epitaxy (CBE) at 430°C using gold particles synthesized using an aerosol method and deposited on InAs (111)B substrates. Further details are described in Ref. [3]. The nanowires have diameters in the range 20-80 nm and they are about 3-4  $\mu\text{m}$  in length. They are known to have the wurzite crystal structure and have hexagonal cross sections.

The substrates used for our manipulation experiments were silicon wafers, capped either by a 330 nm thick thermal oxide layer or with a 120 nm coating of silicon nitride deposited by plasma enhanced chemical vapor deposition (PECVD). Some silicon dioxide substrates were silanised by binding a monolayer of Tridecafluoro- (1,1,2,2)-tetrahydrooctyl-trichlorosilane ( $\text{F}_{13}$ -TCS for short) to the clean thermal oxide [4]. The substrates were patterned with gold dots and location markers using e-beam lithography to allow us identify and re-visit individual nanowires. Nanowires were transferred to our substrates using a piece of clean room wipe in a dry “wipe-on, wipe-off” method.

Our AFM is a Nanoscope IIIa Dimension 3100 from Veeco. For these experiments we used rectangular cantilevers with a nominal spring constant of the order of 30 N/m. The experiments were carried out in an ISO Class 5 cleanroom, in which the temperature and humidity are controlled to 17°C and 24% respectively.

The manipulation procedure has been described in detail in Refs. 1 and 2. Briefly, a conventional tapping mode contour is acquired on the forward scan. On the backward scan the oscillation of the cantilever is quenched, the AFM feedback loop is turned off, and the tip retraces the contour measured on the forward scan, but with a user-selected vertical offset. This offset can be tuned to select different normal forces between tip and substrate, and this force is slowly increased while scanning over a target wire until movement is observed. The scanning speed of the tip during manipulation was in the range 1-3  $\mu\text{m}/\text{sec}$  in all of our experiments.

Static friction measurements are made by pushing on one end of the wire only, so that the end moves but an appreciable portion of the wire does not. Multiple pushes are used to bend the wire into as tight a curve as possible, without breaking it or moving the whole wire across the surface. Sliding friction is measured by pushing the centre of the wire perpendicular to the wire axis, so that it translates sideways without rotating and all parts of the wire have the same velocity with respect to the surface.

The friction force per unit length was determined from the radius of curvature of the bent NW after manipulation using a method developed by our group [1,2]. The radius of curvature is calculated using software which fits an optimized curve to the locus of pixels along the backbone of the nanowire, thus avoiding errors due to tip-sample convolution. In convenient units the friction force per unit length is given by:

$$\frac{F}{(pN/nm)} = \frac{5000\sqrt{3}}{288} \frac{E}{GPa} \frac{(D/nm)^4}{(R/nm)^3} \quad (1)$$

where  $F$  is the frictional force in pN/nm,  $E$  is the Young's modulus in GPa,  $D$  is the distance across the flats of the hexagon in nm, and  $R$  is the radius of curvature at the most tightly bent part of the wire, also in nm. For the Young's modulus we have used the bulk value for InAs, 58 GPa. This is almost certainly incorrect, since the crystal structure of our wires is wurzite, not zinc-blende as in the bulk material, but theoretical considerations suggest the error is likely to be small [5] and will only add a constant offset to the data plotted below.

## Results and Discussion

Figure 1 shows an example of a static friction experiment where a relatively thin 25 nm diameter nanowire is manipulated on a silanised silicon dioxide substrate. The first attempts to push it into a most bent state causes the wire to break. Subsequent pushes bend one of the segments resulting from the break into a tight "U" shape.

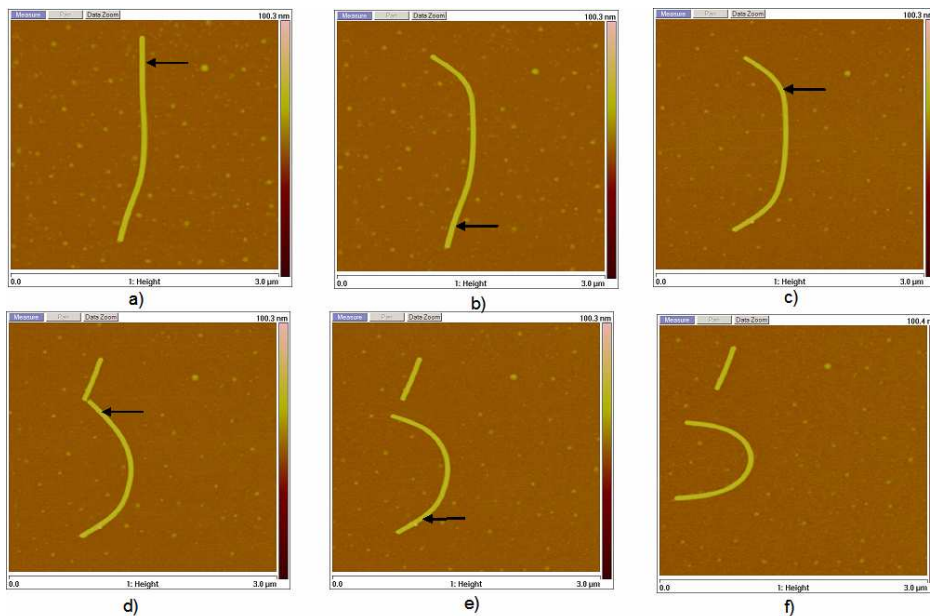


Figure 1. A static friction experiment on a 25 nm diameter wire on a silanised silicon dioxide substrate. The arrows show the position and direction of the push applied to the wire at each stage of the manipulation.

When comparing sliding and static friction it is highly useful to perform both sorts of experiment on the same wire. This ensures that the comparison is made for exactly the same contact geometry, and it avoids differences caused by variations in the surface structure or inhomogeneities in the surface chemical composition. Figure 2 shows a typical experiment performed on a 35 nm diameter NW on a silanised substrate. The total manipulation sequence was longer and here several steps have been omitted for the sake of clarity.

The wire was brought to the bent position shown in Fig. 2a. It was first opened up to the approximately straight state shown in Fig. 2b. This was followed by steps c)-e) in which the wire is translated across the surface while maintaining a constant shape determined by sliding friction. Newer images are shifted with respect to the initial one in order to keep the nanowire centered. After sliding, the wire was bent at one end with the result shown in Fig. 2f where the curvature is determined by static friction. We can clearly see how the radius of curvature of the wire when under the influence of static friction is smaller than the radius of curvature after bending by sliding friction, and from Eqn. 1 it follows that the static friction force per unit length is higher than for sliding friction.

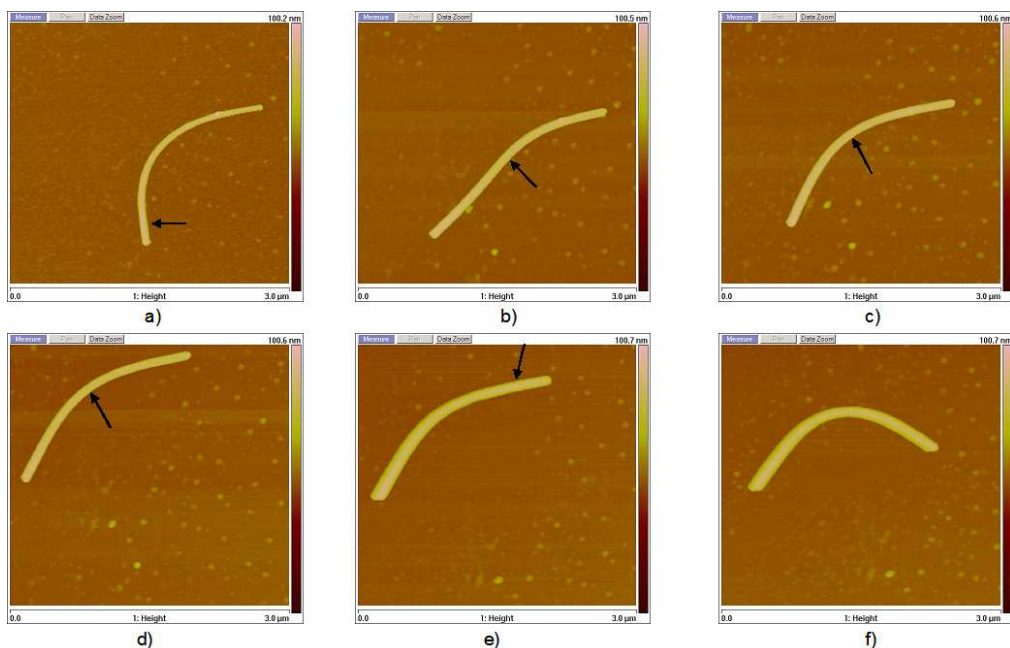


Figure 2. A manipulation experiment on a 35 nm diameter nanowire on a silanised silicon/silicon dioxide substrate.

From manipulation experiments like those shown in Figs. 1 and 2 we have collated sliding and static friction values for a wide range of nanowire diameters on the three different substrates. The results are shown in Figure 3.

We observe the same general trends and features on the oxide and silanised surface as were seen for InAs nanowires deposited on the nitride substrate in Ref. 2. For large diameter wires the clear difference between sliding and static friction, two up to three orders of magnitude can once again be seen. For wires below around 40 nm diameter the sliding friction values mix with those for static friction on all three substrates. We take this as a sign that the smaller wires move by a stick-slip mechanism in which their curvature is determined by the static friction that prevails during the stick phase of the motion.

The static friction values on the oxide and silanised surfaces follow the upward trend in the static data on the nitride surface. This could be due to a systematic change in the Young's modulus with nanowire diameter - in this case a tenfold increase in the Young's modulus would be required to explain the observed decrease in apparent friction if it were due to this effect alone. Such a change is possible, but cannot be accounted for by simple models involving, say, a stiff oxide shell around the wire [2]. An additional factor is that the contact pressure may vary if the Van der Waals force holding the wires to the surface increases sufficiently fast as the nanowire diameter grows. This would suggest a macroscopic-like variation in the friction coefficient with normal force.

A relatively large spread in the data was observed on the oxide and silanised surfaces but is not so pronounced as for nitride. However on silicon nitride we have investigated a much larger number of wires which accentuates the appearance of the spread in the graph. Once again the spread reduces for larger nanowires. It is important to reiterate that this spread is an ensemble variation: for any single wire, repeated measurements of friction over several pushes will give in the worst case a factor of two variation in the measured value, but usually much less.

Perhaps the most dramatic aspect of the graph is the transition to stick-slip motion which appears to occur at roughly the same 40 nm diameter on all three substrates, even on the silanised  $\text{SiO}_2$ , where the absence of water film might be expected to shift a threshold determined by, say, the contact pressure.

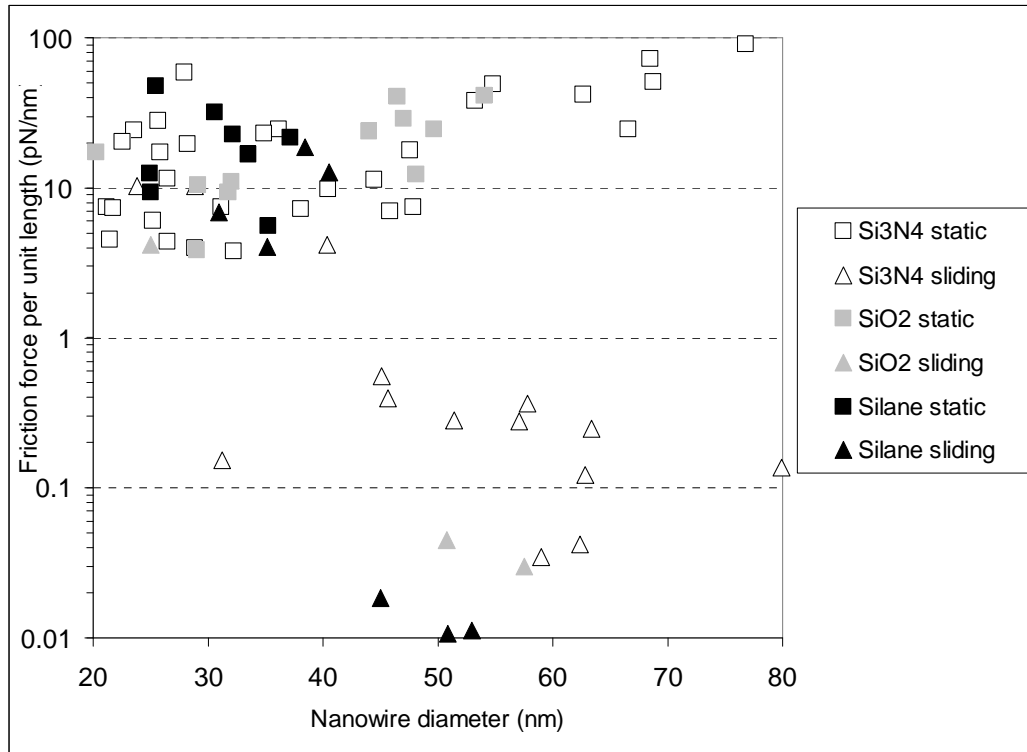


Figure 3. Friction force per unit length vs. NW diameter for InAs NWs deposited on Si/SiO<sub>2</sub>, silanized SiO<sub>2</sub> and Si<sub>3</sub>N<sub>4</sub> substrates.

Similar transitions to stick-slip motion have been observed on all length scales from the atomic up to the large-scale macroscopic. In point contacts stick-slip is governed by the generation of phonons and the individual slips are over a whole number of lattice spacings. In macroscopic friction the stick-slip cycle is determined by the dynamic elastic responses of the two materials in contact and the slips can be of any size. At small length scales the transition from pure sliding to stick-slip motion has been observed as a function of applied load [6], the scan speed or the scan direction with respect to crystallographic directions [7], but in our experiments only the load - set by the Van der Waals attraction of the wire to the surface - is changed.

It is also possible for dynamic crystallization and remelting of a thin adsorbed liquid film to also drive the transition to stick-slip motion [8,9]. Most surfaces at room temperature and pressure have such a film of adsorbed water, and it is possible that this film affects our friction measurements. However, the fact that we see very similar results on the strongly hydrophobic silanised surface and on the hydrophilic oxide and nitride surfaces suggests strongly that this is not the case.

In our work the transition to stick-slip motion seems to be a purely size-related effect. It is particularly intriguing that the transition occurs at about 40 nm diameter on all three substrates. Transport measurements have shown that at 40 nm the zero bias conductivity of ungated wires drops substantially [10], either due to a quenching of dopant ionization, or because a surface conduction channel is lost as the wire shrinks. It is tempting therefore to

speculate on potential electronic contributions to the friction, which would be expected to change as the size threshold for wire conductivity is reached. However, more detailed experiments are needed to confirm this supposition.

The silanised substrate has several properties which distinguish it from the oxide and nitride surfaces. The first is that for larger nanowires sliding friction on the silanised surface is the lowest of all the three substrates studied. One consequence of this is that when trying to push nanowires into tight curves by manipulating one end at a time, they sometimes spring open again. This shows that in the presence of very low sliding friction it is possible to elude the grasp of static friction for a longer period of time. A second consequence is that we can't perform static friction experiments at all for wires more than 40 nm in diameter because we always move the whole wire. With longer wires than we had available for these experiments should be possible to extend the measurements of static friction to larger diameters. Finally, the static friction we are able to measure on the silanised surface is rather similar to that measured on the other two surfaces. At first sight this is rather surprising, as silanised surfaces are widely used as release agents and where low adhesion and stiction is required. However, this is just a reminder that although the two are related, low adhesion does not necessarily mean low friction.

Finally, it is worth noting that the static friction is remarkably similar on all three substrates. The mechanism for static friction is in all our cases unknown, but the similarity in the data suggests that it may be very similar on all three substrates.

## Conclusions

We have investigated static and sliding friction between InAs nanowires and three different substrates:  $\text{SiO}_2$ , silanised  $\text{SiO}_2$  and  $\text{Si}_3\text{N}_4$ . On all three substrates thick wires showed a difference between sliding and static friction of up to three orders of magnitude - a behaviour that is usually associated with atomic-scale point contacts. In addition, the three surfaces all showed a transition to stick-slip motion below a diameter of around 40 nm. The similarity between the results from the hydrophobic nitride surface and the hydrophilic oxide and nitride substrates strongly suggest that the condensed water layer that must be present on the oxide and nitride surfaces does not significantly affect the friction we observe. An increase in static friction by a factor of ten is observed as the nanowire diameter is varied from 20 to 80 nm. This may be due to a change in the wires' Young's modulus with size, but it seems likely that this is not the sole cause. In addition, a variation of the friction force with the contact pressure seems to take place, which is usually taken as a sign of macroscopic friction. Our samples display characteristics of atomic-scale and macroscopic friction, as is appropriate for a mesoscopic system.

## References

- [1] M. Bordag, A. Ribayrol, G. Conache, L. E. Fröberg, S. Gray, L. Samuelson, L. Montelius and H. Pettersson 2007 *Small* **3** 1398
- [2] G Conache, S Gray, A Ribayrol, L E Fröberg, L Samuelson, H Pettersson, and L Montelius, *Friction measurements of InAs nanowires on Si<sub>3</sub>N<sub>4</sub> substrates by AFM manipulation*. Submitted to *Small*.
- [3] Bjork M T, Ohlsson B J, Sass T, Persson A I, Thelander C, Magnusson M H, Deppert K, Wallenberg L R and Samuelson L 2002 *Applied Physics Letters* **80** 1058
- [4] M Beck, M Graczyk, I Maximov, E-L Sarwe, TGI Ling, M Keil, L Montelius 2002 *Micro electronic engineering* **61-62** 441
- [5] R. Martin, *Phys. Rev. B.* **1972**, 6, 4546
- [6] A Socoliuc, R Bennewitz, E Gnecco, E Meyer 2004 *Phys. Rev. Lett.* **92** 134301
- [7] R W Carpick, M Salmeron, 1997 *Chem. Rev.* **97** 1163
- [8] M. O. Robbins and E. D. Smith, 1996 *Langmuir* **12**, 4543
- [9] G. He, M. H. Müser and M. O. Robbins, 1994, *Science* **284** 1650
- [10] C Thelander, M T Björk, M W Larsson, A E Hansen, L R Wallenberg, L Samuelson 2004 *Solid State Communications* **131** 573